






Photoswitchable block copolymers based on main chain α -bisimines†

Linh Duy Thai, ^{a,b,c} Thiago R. Guimaraes, ^{*a,b} Sebastian Spann,^{e,f}
Anja S. Goldmann,^{a,b} Dmitri Golberg, ^{a,b} Hatice Mutlu ^{*c,d} and
Christopher Barner-Kowollik ^{*a,b,c}

We introduce linear diblock copolymers (BCPs) consisting of readily accessible and photoswitchable α -bisimine units in the polymer backbone. The BCPs are prepared *via* a combination of activators regenerated by electron transfer (ARGET) atom transfer radical polymerization (ATRP) and head-to-tail acyclic diene metathesis (ADMET) polymerization. The selective head-to-tail ADMET polymerization of α -bisimine-based asymmetrical monomers in the presence of macro-chain stoppers allows for the construction of well-defined block copolymers. Acrylate-endcapped polystyrenes synthesized from ARGET ATRP and commercial poly(ethylene glycol) methyl ether acrylate were used as macro-chain stoppers. ¹H NMR spectroscopy and Size-Exclusion Chromatography (SEC) confirmed the light-responsive properties of the resulting block copolymers (BCPs) in solution. An unambiguous reversible (Z,Z)/(E,E)-isomerization of the α -bisimines was observed for PS- and PEG-based BCPs upon UV irradiation ($\lambda_{\text{max}} = 254$ nm). The advanced synthetic approach paves the way towards the preparation of efficient light-responsive materials, where in-chain morphological changes are required.

Introduction

Block copolymers (BCPs) are a unique type of polymer, where the chemical and/or physical properties of different and incompatible blocks can be fused. Due their incompatibility, BCPs can undergo microphase separation to generate nanostructured materials.¹ In dispersed systems, the assemblies of BCPs ranges from spheres to cylinders and vesicles, while BCP thin films can constitute variable nano-scale morphologies

including spheres, cylinders, lamella or gyroids.^{1,2} When equipped with a stimuli-responsive function, these static nanostructures can become dynamic and controllable, allowing switching between ordered structures. Such stimuli-responsive materials have found key applications in nanotechnology and nanomedicine.^{3–5}

Among various types of stimuli, light is perhaps the most ideal by virtue of its clean and traceless control with excellent spatiotemporal resolution. As a result, the development of light-responsive BCPs has become a frontier in the field of polymer chemistry.^{6,7} Several types of photo-responsive groups have been discovered and used in synthetic macromolecular systems, namely azobenzenes,^{8,9} spiropyrans,¹⁰ *o*-nitrobenzyl esters^{11,12} or donor–acceptor Stenhouse adducts (DASA).¹³ In BCPs, such groups can be incorporated into the main chain of one block¹⁴ or as a pendant group¹⁵ or at the block junctions.¹⁶ Depending on the nature of the photochemical reaction, *e.g.*, reversible isomerization or irreversible cleavage, the location of such moieties in the polymer chain can have a critical impact on the behavior of the resulting BCPs when irradiated, including the transformation of polymer morphologies. A plethora of polymerization techniques has been employed to produce such BCPs. These strategies include living polymerization,¹⁷ reversible-deactivation radical polymerization (RDRP) (*e.g.*, Atom Transfer Radical Polymerization (ATRP),^{18,19} Reversible Addition–Fragmentation Chain-Transfer (RAFT)²⁰ polymerization and chain-growth

^aSchool of Chemistry and Physics, Queensland University of Technology (QUT), 2 George Street, Brisbane, QLD 4000, Australia.

E-mail: christopher.barnerkowollik@qut.edu.au, thiago.rodriuesguimaraes@qut.edu.au

^bCentre for Materials Science, Queensland University of Technology (QUT), 2 George Street, Brisbane, QLD 4000, Australia

^cInstitute of Nanotechnology, Karlsruhe Institute of Technology (KIT), Hermann-von-Helmholtz-Platz 1, 76344 Eggenstein-Leopoldshafen, Germany.

E-mail: christopher.barner-kowollik@kit.edu

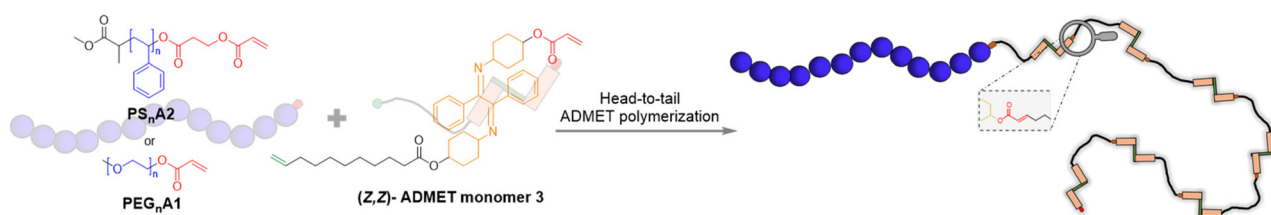
^dSoft Matter Synthesis Laboratory, Karlsruhe Institute of Technology (KIT), Hermann-von-Helmholtz-Platz 1, 76344 Eggenstein-Leopoldshafen, Germany.

E-mail: hatice.mutlu@kit.edu

^eInstitute for Biological Interfaces 4 (IBG-4), Karlsruhe Institute of Technology (KIT), Hermann-von-Helmholtz-Platz 1, 76344 Eggenstein-Leopoldshafen, Germany

^fInstitute of Organic Chemistry, Karlsruhe Institute of Technology (KIT), Fritz-Haber-Weg 6, 76131 Karlsruhe, Germany

† Electronic supplementary information (ESI) available: Experimental methods, SEC, NMR of small molecules and polymers. See DOI: <https://doi.org/10.1039/d2py00994c>



Scheme 1 Synthetic strategy towards block copolymers containing photoswitchable α -bisimine groups in the backbone.

polymerization (e.g., Ring-Opening Metathesis Polymerization (ROMP)²¹). In addition, BCPs have been synthesized *via* the combination of these strategies¹⁴ as well as *via* click chemistry.²²

Despite a large library of existing photo-sensitive molecules, it appears the integration of azobenzenes into BCPs dominates the landscape, probably owing to their properties, e.g., light-induced reversible *trans/cis*-isomerization, crystallinity and responsiveness towards linearly polarized light (LPL).^{23–31} Nevertheless, among azobenzene-based BCPs, the common design strategy is to place the azo-group on the side chain.^{27,30,31} Reports that incorporate azobenzene into the polymer backbone are very scarce, especially for linear diblock copolymers, possibly because of the limited choice of suitable polymerization techniques coupled with the laborious synthetic access to the corresponding light-sensitive monomers.^{32,33} Furthermore, in studies that aimed at the morphological manipulation of azobenzene-containing BCP thin films, the light-driven alteration of the initial nanostructure was typically not drastic. Often observed for such systems was the reorientation of nanocylinders upon the light-driven *trans/cis*-isomerization of the azo group.^{24–26} Even when the structural reorganization was reversible, irradiation under heating or long annealing times after irradiation were usually required.²⁶ Those characteristics are not ideal for future applications in photodynamic nanolithography. Therefore, we submit that there is a critical need for identifying new and efficient photo-switches that can be used for such applications.

On the one hand, imines or Schiff bases are common entities in coordination chemistry, where they are widely used as a ligand based on their capability to form complexes with metal ions.^{34,35} These entities are also known for their covalent dynamic chemistry, e.g., dynamic imine exchange reactions.³⁶ A substantial number of imines are sensitive to aqueous acidic environments and readily cleaved to the corresponding aldehydes/ketones and amines. In addition, imine bonds are prevalent in biomolecules, such as proteins. In polymer chemistry, those attributes have been harnessed to generate polymers with self-healing,^{37,38} mechanical tunable,^{37,39} and pH-responsive^{40,41} properties. pH-sensitive features can be beneficial for the release of drugs encapsulated in nanocapsules due to the local acidic environment in tumor/cancer cells.⁴²

On the other hand, imines, especially chiral aromatic (e.g., benzil) imines, have been recognized as potential candidates

for molecular motors due to their photo-driven *E/Z* isomerization characteristic.^{43,44} Whereas the light-induced *E/Z* isomerization of imines has been known for almost 70 years,⁴⁵ this light-responsive feature has yet to be exploited in polymer science. In fact, there are only very few examples for the utilization of light-responsive imines in polymer science. In 2016, in collaboration with the group of Lehn, we reported an α -bisimine-based dual-stimuli-sensitive polymer *via* ADMET polymerization.⁴⁶ The light-responsive α -bisimine used therein displayed a reversible isomerization between the (*Z,Z*)-thermal dynamically stable configuration and (*E,E*)-configuration. Size Exclusion Chromatography (SEC) and Dynamic Light Scattering (DLS) studies revealed a reversible change in hydrodynamic volume of the homopolymer upon 254 nm irradiation. Such a change was rationalized by the lower rotation energy barrier around the C–C bond (in the –N=C–C=N– system) of the resulting metastable (*E,E*)- α -bisimine repeating unit.⁴⁶

In order to expand the unexplored toolbox of such imine-based photoswitches, we herein report the synthesis and UV-irradiation of linear diblock copolymers that feature α -bisimines as photoswitches in the main chain of one block and poly(styrene) (PS_nA2) or poly(ethylene glycol) (PEG_nA1) as the second block (Scheme 1). Based on the highly selective cross-metathesis reaction between acrylate and alkene functional groups *via* catalysis of a Hoveyda–Grubbs 2nd generation catalyst, ADMET polymerization of the α -acrylate/ ω -ene difunctional monomer 3 in the presence of acrylate-end functionalized PS or PEG afforded the desired linear diblock copolymers (Scheme 1). It is expected that the embedding of the photoswitch, *i.e.*, the α -bisimine units, into the polymer backbone rather than onto the side chain will critically affect the photodynamic properties of the respective block copolymers under UV-irradiation. The simple and straightforward synthesis of the asymmetric α -bisimine-based monomer will also be an excellent choice for future studies that require main-chain photo-sensitive groups.

Experimental section

Materials

Benzil (Alfa Aesar, 98%), *trans*-4-aminocyclohexanol (Apollo Scientific UK, 95%), 10-undecenoyl chloride (TCI, 98%), tri-

ethylamine (Sigma Aldrich, 99.5%), acryloyl chloride (Sigma Aldrich, 97%), Styrene (Sigma Aldrich, 99.9%), copper(I) bromide (Sigma Aldrich, 99.9%), 2-carboxyethyl acrylate (Sigma Aldrich), methyl 2-bromopropionate (MBP) (Sigma Aldrich, 98%), polyethylene glycol methyl ether acrylate ($M_n = 2000$ g mol⁻¹, Sigma Aldrich, **PEG₄₆A1**), tris[2-(dimethylamino)ethyl]amine (Me₆TREN) (Sigma Aldrich, 97%), tin(II) 2-ethylhexanoate (Sn(EH)₂) (Sigma Aldrich), Hoveyda–Grubbs catalyst 2nd generation (Sigma Aldrich, 97%), ethyl vinyl ether (Sigma Aldrich, >99%), cesium carbonate (TCI, >98%), *N,N*-dimethylformamide (Acros Organics, 99.8%, anhydrous), chloroform (Acros Organics, 99.9%, anhydrous), dichloromethane (DCM) (Acros Organics, 99.9%, anhydrous), *p*-xylene (Sigma-Aldrich, 99%). All chemicals and solvents were used without any further purification unless specified.

Synthesis of bisimine diol 1

Bisimine diol **1** was synthesized based on the protocol described in the literature.⁴⁶ Under inert atmosphere, benzil (20 g, 0.095 mol, 1.0 equiv.) and *trans*-4-aminocyclohexanol (23 g, 0.20 mol, 2.1 equiv.) were added to 60 mL of degassed *p*-xylene. The reaction was carried out under reflux for 48 h. Upon completion, the reaction mixture was cooled to ambient temperature and acetone was added. After 30 min of stirring, the mixture was filtered and washed 3 times with acetone to obtain α -bisimine diol **1** (25 g, white or yellow powder/solid, 65% yield).

Synthesis of mono-ol 2

Bisimine diol **1** (4.0 g, 9.9 mmol, 1.1 equiv.) and triethyl amine (Et₃N) (1.24 mL, 8.9 mmol, 1.0 equiv.) were dissolved in 120 mL of chloroform at 60 °C. Upon dissolution, the heat was turned off and a solution of 10-undecenoyl chloride (1.41 mL, 9.9 mmol, 1.0 equiv.) in 10 mL chloroform (1.0 M) was added in a dropwise manner to the previous solution. The reaction was stopped after 36 h. Upon completion, the mixture was washed with water and brine. The organic layer was dried over Na₂SO₄, and the solvent was removed under reduced pressure. The residue was purified by flash column chromatography (EtOAc/*n*-hexane, 1 : 1, v/v) to obtain 2.7 g mono-ol **2** (48% yield) as yellow viscous oil.

Synthesis of ADMET monomer 3

Mono-ol **2** (2.0 g, 3.50 mmol, 1 equiv.) and Et₃N (0.73 mL, 5.26 mmol, 1.5 equiv.) were dissolved in 7.0 mL of dichloromethane. After the solution reached 0 °C, acryloyl chloride (0.42 mL, 5.3 mmol, 1.5 equiv.) in 5.3 mL dichloromethane was slowly added. The temperature was maintained at 0 °C for about 1 h before being allowed to reach ambient temperature. After 24 h, the mixture was diluted in dichloromethane and washed with brine. The organic layer was subsequently dried with Na₂SO₄ and the solvent was removed under reduced pressure. The residue was purified by flash column chromatography (EtOAc/*n*-hexane, 1 : 9, v/v) to obtain 1.7 g monomer **3** (78% yield) as yellow viscous oil.

ARGET ATRP synthesis of PS_nBr polymers

The synthesis protocol was adopted from the literature.⁴⁷ Copper bromide (Cu(I)Br) was purified by a procedure described in the literature.⁴⁸ Styrene (St) and methyl 2-bromopropionate (MBP) was injected into a 25 mL-Schlenk tube charged with a magnetic stirring bar and subsequently percolated with N₂ (g). Meanwhile, a solution of Cu(I)Br, tris[2-(dimethylamino)ethyl]amine (Me₆TREN), and tin(II) 2-ethylhexanoate (Sn(EH)₂) in styrene was percolated with N₂ in a separated flask. Subsequently, the solution was injected to the previous Schlenk tube under N₂ atmosphere. The reaction commenced when the Schlenk tube was immersed in a preheated oil bath at 90 °C. The reaction was stopped when the desired monomer conversion was reached as assessed by ¹H NMR spectroscopy. During the synthesis of **PS₇₀Br**, **PS₁₁₅Br** and **PS₂₃₀Br**, the final [St]/[MBP] ratios were 100, 200 and 400, respectively. In all cases, the molar ratios of Sn(EH)₂ and Me₆TREN to MBP were both 0.1 and the molar ratio of Cu(I)Br to styrene was 50 ppm. After the reaction finished, the solution was diluted in THF and passed through a short neutral alumina column to remove the Cu(I) complex. The solvent was subsequently removed under reduced pressure. The residue was dissolved in THF and precipitated in cold MeOH, filtered and dried under vacuum at 40 °C to obtain the desired polymer.

Post-polymerization modification of PS_nBr polymers

In a typical experiment, 2-carboxyethyl acrylate (68 μ L, 0.57 mmol, 4.0 equiv.) was dissolved in DMF, followed by the addition of Cs₂CO₃ (93 mg, 0.29 mmol, 2.0 equiv.). Subsequently, **PS₇₀Br** (1000 mg, 0.14 mmol, 1.0 equiv.) was slowly added to the mixture. The reaction was carried out at ambient temperature for 48 h. Upon completion, the reaction solution was diluted in ethyl acetate and was washed with water (3 times). The organic phase was dried with MgSO₄ and the solvent was evaporated under reduced pressure. Subsequently, the residue was dissolved in THF and precipitated in cold MeOH, followed by filtration and vacuum drying at 40 °C to obtain the product as white powder.

Synthesis of photoresponsive block copolymers

ADMET monomer **3** (0.5 M) and macro-chain stopper (**PS_nA2** or **PEG₄₆A1**) were dissolved in dichloromethane in a Schlenk tube. The designed degree of polymerization in the ADMET block was calculated based on the molar ratio of the monomer and the acrylate functional group of the macro-chain stopper. Subsequently, Hoveyda–Grubbs (2nd generation) catalyst (3 mol%, with respect to the mole the monomer **3**) was added and the reaction mixture was immersed in a preheated oil bath at 40 °C. The valve of the Schlenk tube was gently opened from time to time to release the generated ethylene gas. After 3 h, another batch of the catalyst (3 mol%) was added. The conversion was monitored by ¹H NMR spectroscopy and SEC. Ethyl vinyl ether was added 30 min before the reaction was stopped to quench the catalyst. The reaction mixture was subsequently

precipitated in methanol, followed by centrifugation and vacuum drying at 40 °C.

UV-irradiation experiments

The irradiation study was monitored by ^1H NMR spectroscopy and SEC for the block copolymer samples. Solutions of block copolymers ($\text{PEG}_{46}\text{ADMET}_{20}$, 1.0 gL $^{-1}$, and $\text{PS}_{115}\text{ADMET}_{10}$, 2.0 gL $^{-1}$) in THF- d_8 (for ^1H NMR study) or in HPLC THF (for SEC study) and α -bisimine diol **1** (1.24 mM in methanol- d_4) were contained in quartz NMR tubes. The solutions were placed approximately 15 cm (4 cm, in the case of bisimine diol **1**) from the UV-C-lamp (Osram Puritec HNS, 36 W, λ_{max} = 254 nm).

Results and discussion

Initially, we focused on the synthesis of asymmetrical α -acrylate/ ω -ene difunctional α -bisimine-based monomer. In the second step, ARGET-ATRP polymerization was conducted, resulting in the Br-end functionalized polystyrene. Upon end-group modification, acrylate-end functionalized polystyrene and commercial $\text{PEG}_{46}\text{A1}$ were used as macro-chain stoppers in the head-to-tail ADMET polymerization of asymmetrical monomer **1**. Subsequently, the light-responsive properties of the resulting block copolymer as well as the α -bisimine small molecule were investigated *via* ^1H NMR spectroscopy and SEC measurements.

Synthesis of ADMET monomer

ADMET monomer **3** (^1H NMR spectrum depicted in Fig. 1) was successfully synthesized *via* a 3-step protocol, including one condensation reaction and two consecutive esterification reactions (Scheme 2A). Bisimine diol **1** was obtained on the gram-

scale with good yield (65%) comparable with the reported value in literature.⁴⁶ Purification of bisimine diol **1** was facile, only requiring washing with acetone. Interestingly, mono-ol **2** was directly obtained with 48% yield from the symmetric diol **1** without the need of protecting one of the two hydroxy groups beforehand. In addition, mono-ol **2** and monomer **3** were stable under the mildly acidic condition of the silica gel column during the purification with flash column chromatography.

Synthesis of PS-based macro-chain stoppers

The macro-chain stoppers were obtained *via* post-polymerization modification of the Br-end group of homopolymers synthesized from ARGET ATRP (Scheme 2B). Initially, we intended to use conventional ATRP for the synthesis of halide-capped homopolymers. However, a significant loss of the halide end-group at moderate monomer conversion was encountered. In fact, the decrease of halide chain-end fidelity in traditional ATRP, due to an elimination reaction, has been reported before, especially for styrene-based polymers.^{47,49} Given the significant importance of preserving the halide-end group for post-polymerization modification, ARGET ATRP was employed. Besides minimizing the undesirable elimination of the halide-end group, the amount of Cu(I) catalyst used in ARGET ATRP can be reduced to ppm levels.⁴⁷ Accordingly, a series of polystyrenes (PS_nBr) with high fidelity of the Br-end group (up to 92%) were synthesized (Table 1). Subsequently, acrylate chain-end macro-chain stoppers ($\text{PS}_n\text{A2}$) were obtained *via* the transformation of the Br-end group of the respective homopolymers. ^1H NMR analysis (Fig. 2A) confirmed the successful end-group modification by the disappearance of magnetic resonance associated with proton **b**, indicating the presence of the Br-end group and the appearance of new magnetic resonances associated with the acrylate-end group. Furthermore, SEC traces show no change in the molecular weight distribution of polymers upon the modification (Fig. 2B).

Synthesis of photoresponsive block copolymers

Next, we focused on the preparation of light responsive BCP *via* head-to-tail ADMET polymerization of monomer **3** and acrylate-end polymers at different ratios (Table 2). Preliminary experiments (results not shown) on ADMET homopolymerization of monomer **3** showed that 3 mol% (with respect to the mole of monomer **3**) of Hoveyda-Grubbs 2nd generation catalyst was required for an efficient polymerization in DCM at 40 °C. Therefore, these conditions were applied for the block copolymer synthesis. To demonstrate the versatility of our system, three acrylate-end functionalized PS with different number average molecular weight ($\text{PS}_{70}\text{A2}$, $\text{PS}_{115}\text{A2}$ and $\text{PS}_{230}\text{A2}$) were employed as macro-chain stoppers in the head-to-tail ADMET polymerization in the presence of monomer **3**.

The results as well as the optimized experimental conditions are summarized in Table 2. SEC traces of the purified block copolymers obtained from $\text{PS}_{70}\text{A2}$ show monomodal peaks with a good shift towards higher molecular weights, indicating the successful preparation of block copolymer

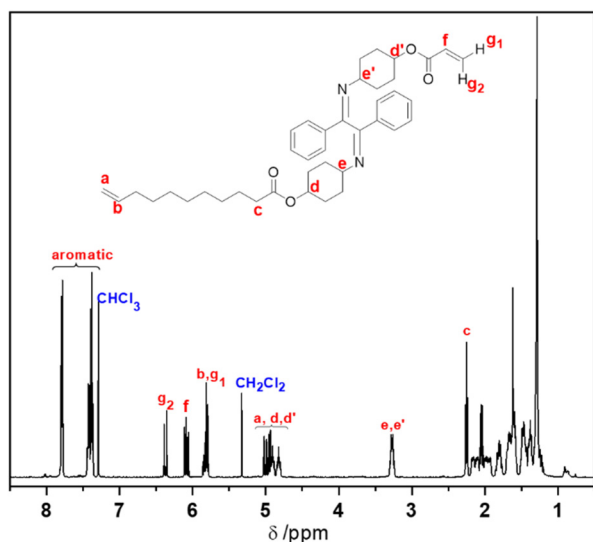
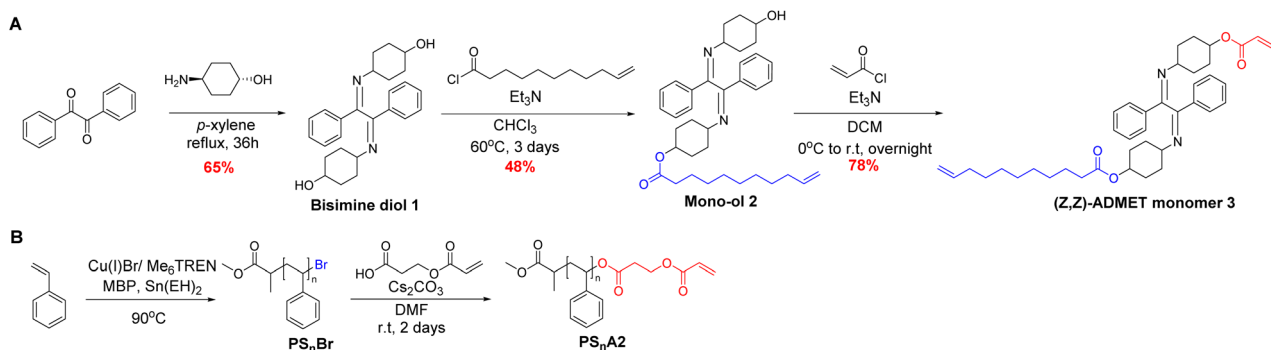


Fig. 1 ^1H NMR spectrum (500 MHz, CDCl_3 , 16 scans) of (Z,Z)-monomer **3**.



Scheme 2 Synthetic route to (Z,Z)-ADMET monomer **3** (A) and macro-chain stopper **PS_nA2** (B).

Table 1 Characterization data of homopolymers synthesized from ARGET ATRP

Polymer ^a	$M_n/g\ mol^{-1}$		D^d	%f ^e (Br)
	NMR ^b	SEC ^c		
PS₇₀Br	7500	8000	1.2	92%
PS₁₁₅Br	12 000	13 000	1.2	92%
PS₂₃₀Br	23 000	26 000	1.2	85%

^a Subscript indicates the degree of polymerization determined by ¹H NMR spectroscopy (500 MHz, CDCl₃, 32 scans). ^b Molecular weight determined by ¹H NMR spectroscopy. ^c Molecular weight determined by THF-SEC, PS calibration standard. ^d $D = M_w/M_n$, determined by SEC. ^e Degree of Br-end group functionalization, determined by ¹H NMR spectroscopy.

(Fig. 3C). The shift towards high molecular weight was also observed with higher MW obtained by varying the molar ratio between monomer **3** and **PS₇₀A2** from 6 to 12 and to 50:1. However a minor ‘tailing’ of SEC-traces was observed for the higher ratios, indicating the presence of some unreacted PS. Monomodal SEC traces were also observed when higher MW **PS₁₁₅A2** (Fig. 3D) was employed. However, in the case of **PS₂₃₀A2** (1:50, with respect to the mole of monomer **3**), SEC traces of the crude sample showed a predominant amount of ADMET homopolymer and unsatisfactory peak shift (Fig. S30 – ESI†). Possibly, for the high M_n macro-chain stopper **PS_nA2** or the growing block copolymer, the coupling catalyzed by Hoveyda–Grubbs 2nd generation catalyst between the macro-chain stopper and the ADMET monomer/oligomer becomes ineffective. This may be associated with the coil conformation of the polymer in the solvent, leading to the acrylate-end group buried within the polymer chains, making it inaccessible to the Hoveyda–Grubbs 2nd generation catalyst. It could be argued that such mechanism would be also observed for low molecular PS-based systems (e.g. **PS₇₀A2**). However, as evidenced by the DOSY NMR spectrum (Fig. 4C) and SEC-traces (Fig. 3C), it is probable that the number of unreacted PS chains is small, indicating that such a mechanism occurs to a much lesser extent for low molecular weight macro-chain stoppers.

In addition to the nonpolar macro-chain stoppers (**PS₇₀A2** and **PS₁₁₅A2**), we also assessed a more polar macro-chain

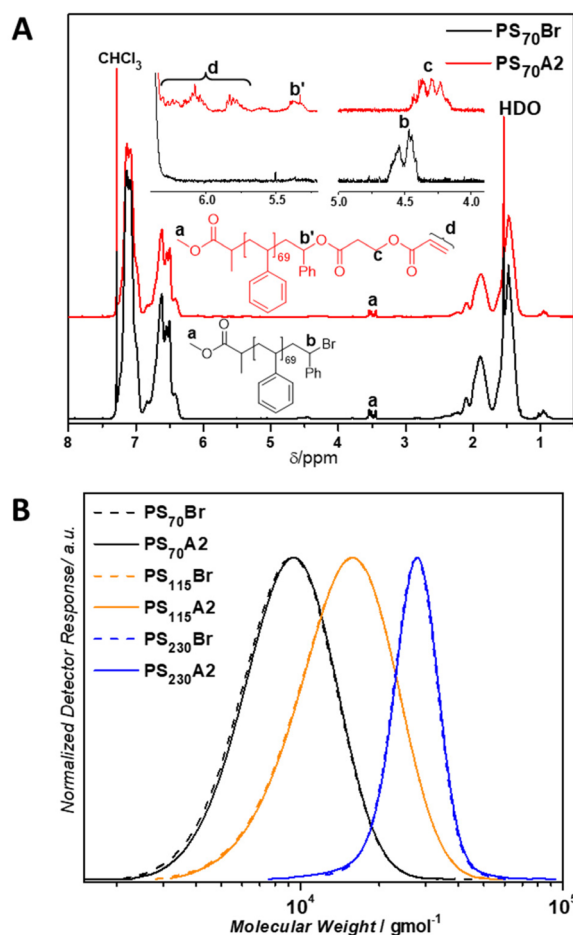


Fig. 2 Comparative ¹H NMR spectra (500 MHz, CDCl₃, 32 scans) of **PS₇₀Br** and **PS₇₀A2** (A) and THF-SEC traces of **PS_nBr** and **PS_nA2** (B), respectively.

stopper, *i.e.*, poly(ethylene glycol) methyl ether acrylate ($M_n = 2000\ g\ mol^{-1}$, denoted **PEG₄₆A1**). The same ADMET polymerization conditions were applied for **PEG₄₆A1**. The SEC traces of the resulting polymer shifted well from that of the initial macro-chain stopper (Fig. 3E), indicating the successful formation of a block copolymer. Considering that α -bisimine

Table 2 Summary of results for block copolymer synthesis experiments

Entry	Block A (macro-chain stopper)			ADMET block			Block copolymer		
	Name ^a	M_n ^b /g mol ⁻¹ /D	$D^c \times 10^{10}$ /m ² s ⁻¹	Target ^d	NMR ^e	SEC ^f	Name ^a	M_n ^b /g mol ⁻¹ /D	$D^c \times 10^{10}$ /m ² s ⁻¹
1	PS ₇₀ A2	8000/1.2	1.31	6	5	3	PS ₇₀ ADMET ₅	10 000/1.3	1.16
2				12	8	5	PS ₇₀ ADMET ₈	12 000/1.5	0.94
3				50	34	11	PS ₇₀ ADMET ₃₄	15 000/1.9	0.79
4	PS ₁₁₅ A2	13 000/1.2	1.15	12	10	4	PS ₁₁₅ ADMET ₁₀	15 000/1.3	0.98
5				50	36	9	PS ₁₁₅ ADMET ₃₆	18 000/1.6	0.67
6	PS ₂₃₀ A2	26 000/1.2	—	50	No chain extension/mixture of BCP and significant amount of ADMET homopolymer				
7	PEG ₄₆ A1	2000/1.1	2.15	12	20	14	PEG ₄₆ ADMET ₂₀	11 000/1.7	1.06

[ADMET monomer 3] = 0.5 mol L⁻¹, 3.0 mol% catalyst, DCM, 40 °C. ^aSubscript indicates degree of polymerization of purified BCPs, determined from ¹H NMR (500 MHz, CDCl₃, 32 scans). ^bFor PS- and PEG-based polymers, M_n was derived from PS and PMMA calibration standard, respectively. ^cBased on DOSY NMR (400 MHz, CDCl₃). ^d[ADMET monomer 3]/[macro-chain stopper]. ^eFor purified BCPs, determined from ¹H NMR. ^fFor purified BCPs, determined from SEC.

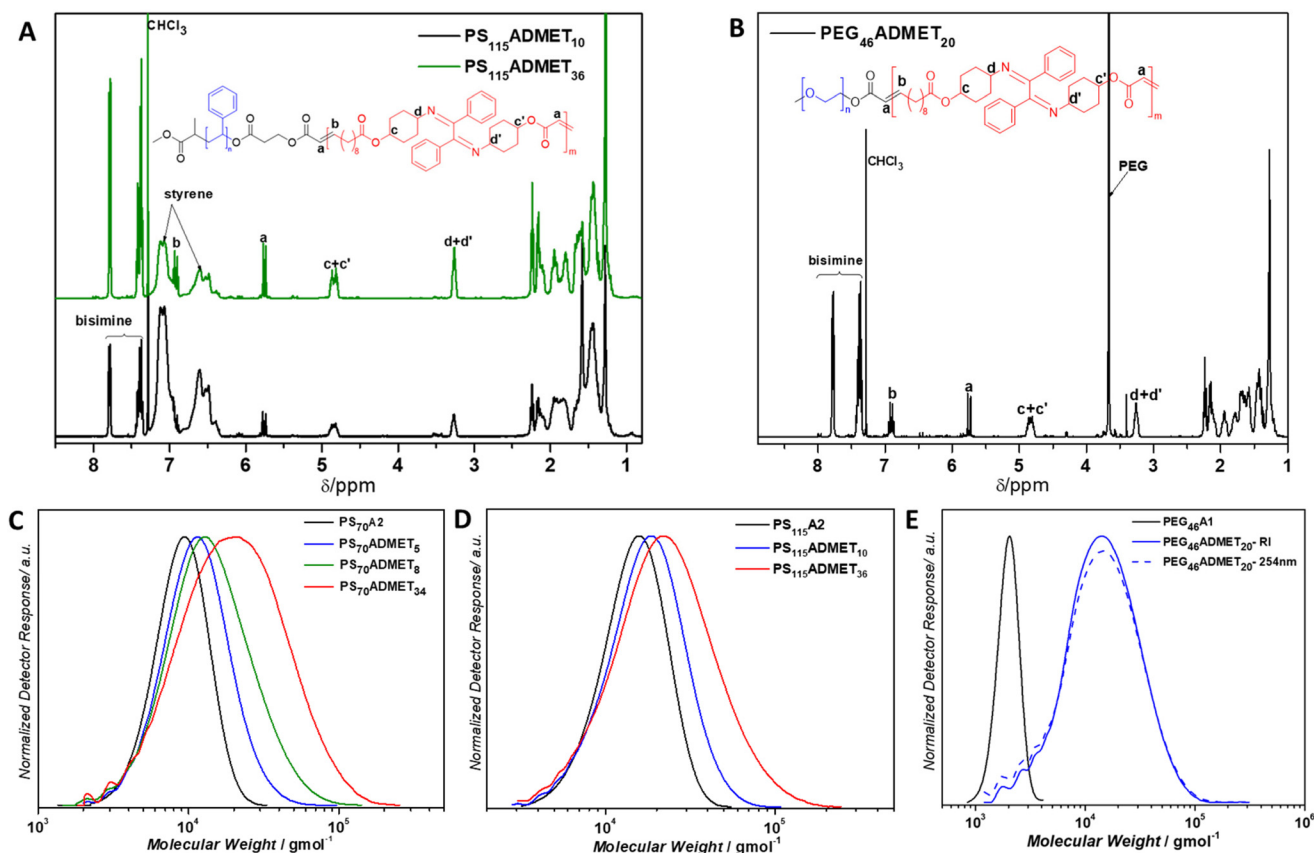


Fig. 3 Stacked ¹H NMR spectra (A) and THF-SEC traces (D) of BCPs based on PS₁₁₅A2; THF-SEC traces (C) of BCPs based on PS₇₀A2; ¹H NMR spectrum (B), THF-SEC traces (E) of BCP based on PEG₄₆A1 macro-chain stopper. ¹H NMR spectra: 500 MHz, CDCl₃, 32 scans; SEC traces: THF, 35 °C.

absorbs UV at 254 nm, while the PEG-adsorption can be neglected, SEC analysis with UV-detector at 254 nm was also conducted. The good overlay between RI and UV (Fig. 3E) indicates the well-distributed presence of α -bisimine within the block copolymer. In addition, the ¹H NMR spectrum shown in Fig. 3B confirms the presence of the PEG and α -bisimine segments.

Critically, DOSY NMR (diffusion ordered spectroscopy) spectra were recorded for selected samples. DOSY has evolved as a complementary technique for the confirmation of successful chain extension in BCP synthesis.^{50,51} In principle, to confirm the formation of diblock copolymers, the magnetic resonances of protons associated with two different blocks covalently linked together should have the same diffusion coeffi-

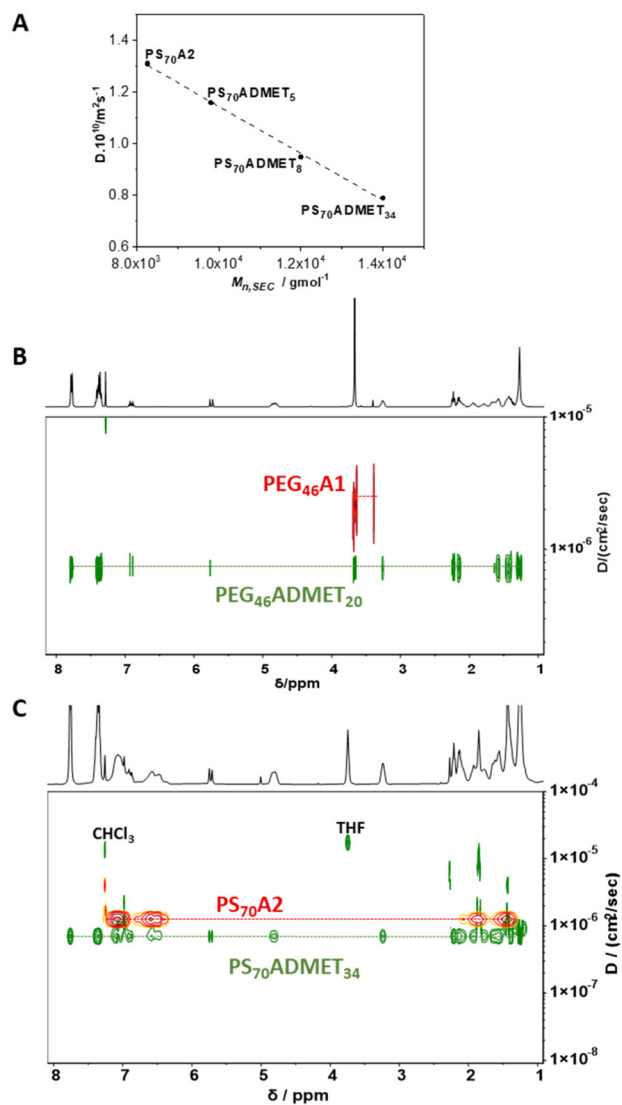


Fig. 4 (A) Plot of D vs. $M_{n,SEC}$ for BCPs based on macro-chain stopper **PS₇₀A2**. The dash line represents the least squares regression line, plotted from the equation: $D/\text{cm}^2 \text{ s}^{-1} = -9.1 \times 10^{-11} M_{n,SEC}/\text{g mol}^{-1} + 2.1 \times 10^{-6}$, $r^2 = 0.997$. (B) Stacked DOSY NMR spectra (400 MHz, THF-*d*₈) of **PEG₄₆A1** and **PEG₄₆ADMET₂₀**. (C) Stacked DOSY NMR spectra (400 MHz, THF-*d*₈) of **PS₇₀A2** and **PS₇₀ADMET₃₄**.

cient. Pleasingly, DOSY returns only one average diffusion coefficient value for each polymer sample (Table 2 and ESI†). As an illustration, the DOSY NMR spectra of macro-chain stopper **PEG₄₆A1** and the corresponding polymer **PEG₄₆ADMET₂₀** are depicted in Fig. 4B. The diffusion coefficients for protons in both segments (PEG and α -bisimine segments) perfectly align and shift to lower values compared to the initial macro-chain stopper **PEG₄₆A1**, implying that the two blocks are covalently connected. Similar results were obtained for PS-based polymers, namely **PS₇₀ADMET₃₄**, as shown in Fig. 4C (additional DOSY NMR spectra of PS-based BCP can be found in the Fig. S23–S28 ESI†). These results are in agreement with those from SEC measurements, confirming the successful

block copolymer formation. Furthermore, it is well-known that the diffusion coefficient D expressed in Stokes–Einstein equation is inversely proportional to the hydrodynamic radius of the solute.^{52,53} In theory, the expected relationship between the diffusion coefficient (D) and the molecular weight (MW) of a solute should be $D \propto \text{MW}^{-1/3}$, assuming a spherical shape of the polymeric solute. To examine such a correlation, the diffusion coefficients gathered for the **PS₇₀A2**-based BCPs were plotted vs. the respective molecular weights determined from SEC (Fig. 4A). In our case, the diffusion coefficient shows a clear linearity with molecular weight, decreasing with the increase in molecular weight of the polymer samples (Fig. 4A). Given the small differences in $M_{n,SEC}$ of these polymers, it is reasonable that a linear dependence between these two parameters is found.⁵⁴

Having a closer look at the ¹H NMR spectra of the BCPs (Fig. 3A and B), the presence of PS-/PEG- and α -bisimine-based components can be clearly observed. Furthermore, due to the selective cross-metathesis between the electron-deficient acrylate and electron-rich alkene, the internal electron deficient double bonds forming in the main chain of the α -bisimine block of the resulting BCPs is evidenced by the multiplicities as well as chemical shifts of the corresponding protons (5.7 and 6.9 ppm, Fig. 3A and B). Such functional groups can facilitate post-polymerization modification of the bisimine block, for example, *via* Michael-addition reaction⁵⁵ or azide-zwitterion cycloaddition,⁵⁶ enabling the synthesis of tailor-made advanced macromolecular structures.

Inspection of Table 2 indicates that the degree of polymerization (DP) for the ADMET block calculated from ¹H NMR spectroscopy and SEC are not in agreement with each other. The discrepancy becomes larger with higher ratios of ADMET monomer. Furthermore, close inspection of the SEC traces of BCPs generated from PS-based macro-chain stoppers (Fig. 3C and D) indicates that the distributions in the lower molecular weight regions of those BCPs show somewhat incomplete shifts from those of the corresponding macro-chain stoppers, especially in the case of **PS₁₁₅ADMET₃₆**, where the degree of polymerization is higher. Such minor ‘tailing’ of molecular weight distribution and the disagreement between NMR-based and SEC-based degree of polymerization likely arise from the backbone of the α -bisimine-based block. Unlike the often-encountered saturated, aliphatic polymeric backbones, the mainchain of the ADMET block in our case constitutes bulky and rigid α -bisimine units (which also have cyclic rings in their structure) as well as internal electron deficient olefin. Consequently, the interaction of the α -bisimine-based block with the stationary phase of the SEC column and with the other block based on polystyrene will be markedly different from that of those saturated, aliphatic backbones. Thus, the use of conventional PS-/PMMA standard calibration curves can lead to incorrect number average molecular weights of such BCPs. Further, as a minor remark on the **PEG₄₆ADMET₂₀** BCP, the degree of polymerization calculated from NMR (DP_{NMR}) is higher than the target (Table 2). However, the ¹H NMR spectrum recorded for the crude (before purification)

showed a similar molar ratio compared to the designed. Therefore, the higher DP_{NMR} for the purified BCP is probably because of the dissolving of BCP that contains higher amount of PEG-block in MeOH used to precipitate the BCP.

Subsequently, the thermal properties of the block copolymer were investigated (Fig. 5). TGA analysis of the block copolymer $\text{PS}_{115}\text{ADMET}_{36}$ showed an onset of thermal degradation under N_2 at 290 °C followed by two degradations with an inflection point at 405 °C (Fig. 5A). This is an expected profile due to the different composition of each segment of the block copolymer. The DSC analysis of the ADMET homopolymer and $\text{PS}_{115}\text{ADMET}_{36}$ block copolymer were also recorded (Fig. 5B). The thermogram for the ADMET homopolymer clearly shows an endothermic transition at 115° indicating the homopolymer's T_g . For the block copolymer, two endothermic peaks corresponding to the glass transition temperature of the polystyrene-based and α -bisimine-based blocks were detected during DSC, suggesting microphase-separation in $\text{PS}_{115}\text{ADMET}_{36}$ (Fig. 5B). The latter results are very promising, emphasizing a high thermal stability for the photoswitchable BCP, alongside their ability to undergo microphase separation – two key requirements for their application in photodynamic nanolithography.

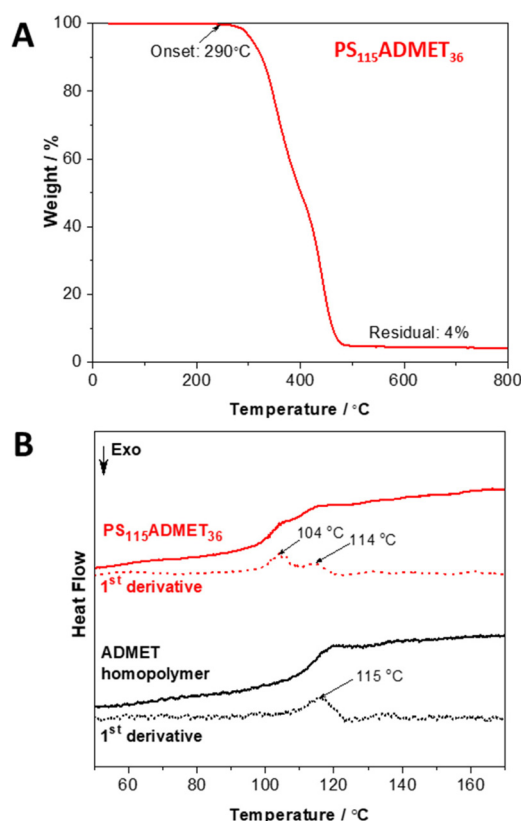


Fig. 5 Thermal properties of $\text{PS}_{115}\text{ADMET}_{36}$. (A) TGA conducted at a heating rate of 20 °C min^{-1} from 30 °C to 800 °C under N_2 and (B) DSC heat flow and first derivative obtained from the 2nd heating ramp at scanning speed of 10 °C min^{-1} in the temperature range from 0 °C to 200 °C.

Irradiation of bisimine diol 1

Prior to carrying out the irradiation experiments on BCPs, we assessed the isomerization of bisimine diol **1** using ^1H NMR spectroscopy. Based on results of our earlier investigation,⁴⁶ $\lambda_{\text{max}} = 254\text{ nm}$ was chosen for the irradiation of a solution of bisimine diol **1** in methanol- d_4 . Inspection of Fig. 6 demonstrates that after 60 min of irradiation, 88% of the initial (Z,Z)-bisimine diol **1** switched to the (E,E)-isomer. The ratio of (Z,Z)/(E,E) isomers was calculated based on the ^1H NMR integral values of peak c' (which appeared upon irradiation) and peak c (Fig. 6). Fig. 6 indicates that an up-field shift of protons **a** and a down-field shift of protons **b** when irradiated at $\lambda_{\text{max}} = 254\text{ nm}$. Furthermore, some changes are observed for other protons in the cyclohexyl rings. Approximately six main resonances in the range of (1.0–2.1) ppm present before the irradiation, corresponding to the remaining 16 protons in the cyclohexyl ring. However, these resonances appear to merge upon irradiation, leading to only 3 main peaks. After 24 h in the dark at ambient temperature (without further irradiation), these NMR resonances revert to their initial positions, indicating that the reversible isomerization of the C=N imine bonds might have an impact on the conformations of the cyclohexyl rings.

Irradiation of BCPs in THF

^1H NMR spectroscopy and SEC were both employed to study the light-responsiveness of $\text{PEG}_{46}\text{ADMET}_{20}$ and $\text{PS}_{115}\text{ADMET}_{10}$

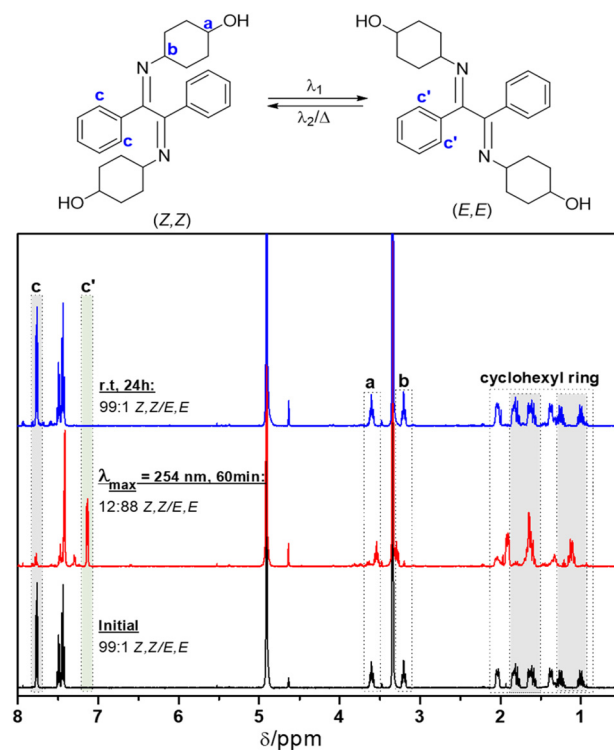


Fig. 6 Stacked ^1H NMR spectra (500 MHz, 16 scans) of bisimine diol **1** in methanol- d_4 recorded at different stages of the irradiation experiment.

upon UV light irradiation. In general, the behavior of the α -bisimine cores installed in the main chain of the BCPs is consistent with that of α -bisimine diol **1** in the NMR study. With $\text{PEG}_{46}\text{ADMET}_{20}$, 75 min of irradiation at $\lambda_{\text{max}} = 254$ nm resulted in 79% of the (*E,E*)-isomer which subsequently reverted to the initial configuration upon thermal back-isomerization at ambient temperature overnight (Fig. 7A). However, we noticed that the irradiation at this wavelength caused some degree of irreversible isomerization of the internal electron deficient double bonds (approximately 30%). The NMR study of $\text{PS}_{115}\text{ADMET}_{10}$ also gave similar results (Fig. 7C). Due to the relatively lower content of α -bisimine units in $\text{PS}_{115}\text{ADMET}_{10}$, the concentration was fixed at 2.0 g L^{-1} instead of 1.0 g L^{-1} as previously employed. Approximately 61% of the (*E,E*)-isomers formed after 20 min of irradiation. Noticeably, the relative intensities of the aromatic protons resonances associated with the α -bisimine units were lost compared to those in the polystyrene block. However, upon thermal reversion at ambient temperature overnight, the initial relative intensities were reestablished.

Next, we proceeded with the SEC study. The data in Fig. 7B indicate that the M_n of $\text{PEG}_{46}\text{ADMET}_{20}$ slightly increases upon UV-C irradiation ($\lambda_{\text{max}} = 254$ nm). Surprisingly, with the reversion (19 h at r.t. in the dark), the molecular weight distribution shifts to lower molecular weight compared to that of the initial sample. The D values and the shape of the curve remained almost unchanged throughout the process. Likely the irreversible isomerization of the internal electron deficient double bond, noted previously in the NMR study, partly contributes to the reduction of the hydrodynamic volume of the coil. It could be also argued that some degree of decomposition of $\text{PEG}_{46}\text{ADMET}_{20}$ triggered by the UV-light is occurring. However, based on the results from the NMR study, apart from the new resonances arising from the solvent, no signs of fragmentation of the polymer chain were observed. Regarding $\text{PS}_{115}\text{ADMET}_{10}$, no significant changes were seen in its SEC traces (Fig. 7D), associated with the lower fraction (33 wt% based on ^1H NMR, Table 2) of the α -bisimine-based block in the $\text{PS}_{115}\text{ADMET}_{10}$ compared to 86 wt% in the $\text{PEG}_{46}\text{ADMET}_{20}$. Therefore, it is reasonable to assume the isomerization of the

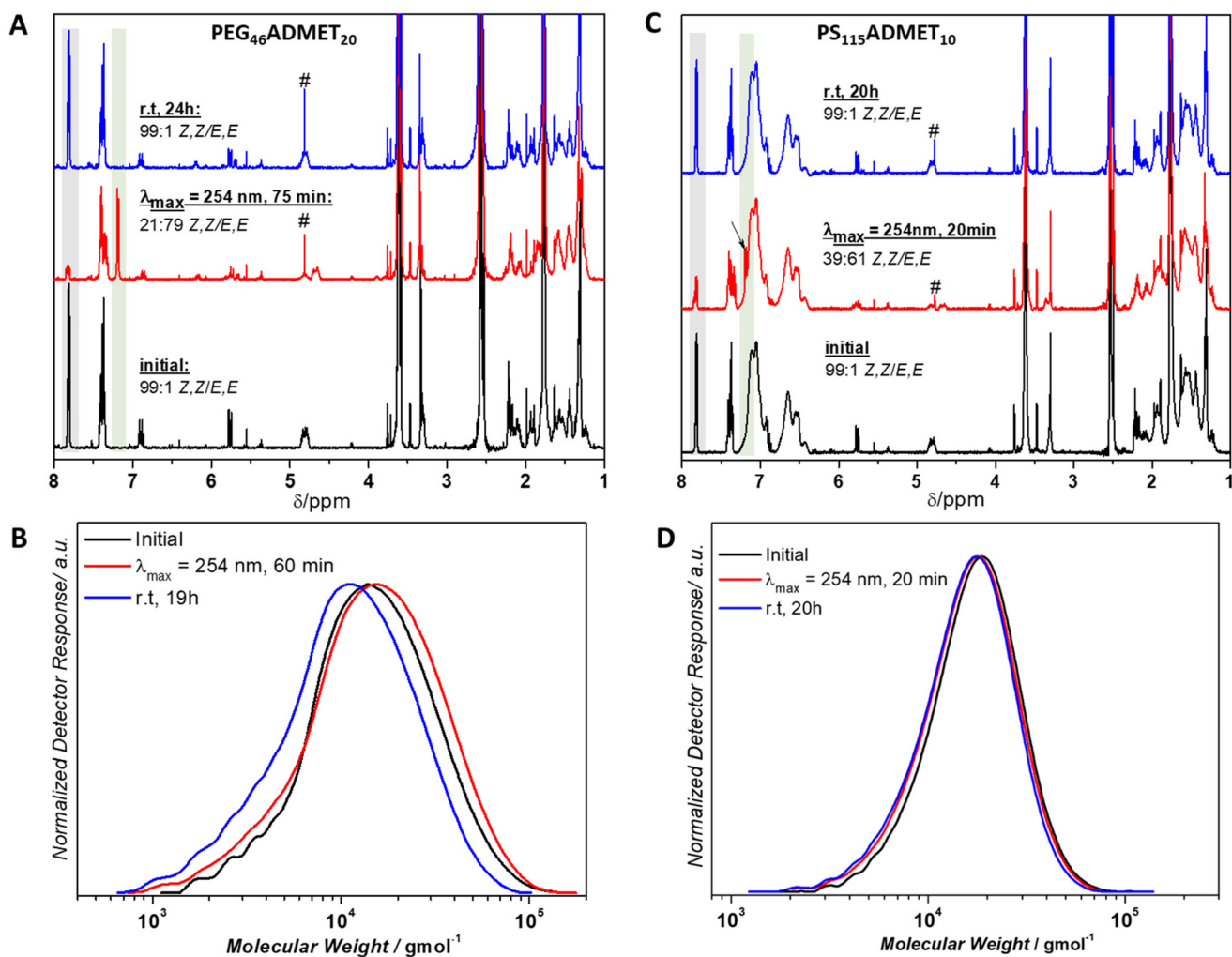


Fig. 7 Stacked ^1H NMR spectra (500 MHz, THF-d_8 , 32 scans) and THF-SEC traces recorded from the irradiation ($\lambda_{\text{max}} = 254$ nm) of $\text{PEG}_{46}\text{ADMET}_{20}$ (A and B) and $\text{PS}_{115}\text{ADMET}_{10}$ (C and D). The resonances marked with # in the NMR spectra are associated with the NMR solvent.

α -bisimine units in **PS**₁₁₅**ADMET**₁₀ caused no significant changes in the hydrodynamic volume of the BCP. Overall, the fully reversible photoisomerization of the α -bisimine units embedded within the main chain of the BCPs was clearly evidenced by the ¹H NMR spectroscopy study, making these light-responsive polymers excellent candidates for applications in photodynamic nanolithography. Due to the amphiphilic nature of **PEG**₄₆**ADMET**₂₀, we also anticipate its utilization as light-responsive self-assemblies forming entity in dispersed media.

Conclusion

We introduce the incorporation of photo-switchable α -bisimine moieties as repeat units into the backbone of linear diblock copolymers. The light-responsive block was covalently linked with either polystyrene block synthesized *via* ATRP or a commercially accessible PEG block. The successful chain extension was validated in a complementary way both *via* SEC and DOSY NMR analysis. Furthermore, thermal analysis, particularly DSC, of one block copolymer sample (**PS**₁₁₅**ADMET**₃₆) indicated microphase-separation. Critically, during the irradiation experiments, solutions of **PEG**₄₆**ADMET**₂₀ and **PS**₁₁₅**ADMET**₁₀ were irradiated at $\lambda_{\max} = 254$ nm and their responses were monitored by ¹H NMR and SEC. The NMR study demonstrated that the (Z,Z)/(E,E) isomerization of the α -bisimine was efficient and fully reversible despite some minor degree of irreversible *trans/cis*-isomerization of the internal electron deficient double bonds under $\lambda_{\max} = 254$ nm irradiation. Perhaps because of such irreversible isomerization at the internal double bonds, the change in the molecular weight distribution of the block copolymers in the SEC study was not completely reversible. Overall, the current work clearly demonstrates the potential of these light-responsive polymeric materials for applications in the field of nanolithography. The PEG-based amphiphilic block copolymer produced in the study may also be applied in dispersed systems where the resulting self-assemblies can interact with light.

Conflicts of interest

There are no conflicts to declare.

Acknowledgements

C. B.-K. and D. G. acknowledge the Australian Research Council (ARC) for funding in the context of their respective Laureate Fellowships enabling their photochemical and microscopy focused research programs as well as QUT's Centre for Materials Science for a grant enabling the current work. C. B.-K. thanks the Karlsruhe Institute of Technology (KIT) for continued funding. The Central Analytical Research Facility (CARF) at QUT is gratefully acknowledged.

References

- 1 L. Leibler, *Macromolecules*, 1980, **13**, 1602–1617.
- 2 A. Blanz, S. P. Armes and A. J. Ryan, *Macromol. Rapid Commun.*, 2009, **30**, 267–277.
- 3 Y. Song, Y. Ding and C. M. Dong, *Wiley Interdiscip. Rev.: Nanomed. Nanobiotechnol.*, 2022, **14**, e1742.
- 4 S. H. Pham, Y. Choi and J. Choi, *Pharmaceutics*, 2020, **12**, 630.
- 5 C.-L. Liu, C.-H. Lin, C.-C. Kuo, S.-T. Lin and W.-C. Chen, *Prog. Polym. Sci.*, 2011, **36**, 603–637.
- 6 M. Zheng and J. Yuan, *Org. Biomol. Chem.*, 2021, **12**, 2210–2221.
- 7 Y. Tang and G. Wang, *J. Photochem. Photobiol., C*, 2021, **47**, 100420.
- 8 C. Fedele, P. Netti and S. Cavalli, *Biomater. Sci.*, 2018, **6**, 990–995.
- 9 L. Rocha, C.-M. Păiuș, A. Luca-Raicu, E. Resmerita, A. Rusu, I.-A. Moleavin, M. Hamel, N. Branza-Nichita and N. Hurduc, *J. Photochem. Photobiol., A*, 2014, **291**, 16–25.
- 10 J. K. Rad, Z. Balzade and A. R. Mahdavian, *J. Photochem. Photobiol., C*, 2022, 100487.
- 11 A. Romano, I. Roppolo, E. Rossegger, S. Schlögl and M. Sangermano, *Materials*, 2020, **13**, 2777.
- 12 M.-F. Tsai, Y.-L. Lo, Y. Soorni, C.-H. Su, S. S. Sivasoorian, J.-Y. Yang and L.-F. Wang, *ACS Appl. Bio Mater.*, 2021, **4**, 3264–3275.
- 13 O. Rifaie-Graham, S. Ulrich, N. F. Galensowske, S. Balog, M. Chami, D. Rentsch, J. R. Hemmer, J. Read de Alaniz, L. F. Boesel and N. Bruns, *J. Am. Chem. Soc.*, 2018, **140**, 8027–8036.
- 14 L. Ding, Y. Li, H. Cang, J. Li, C. Wang and W. Song, *Polymer*, 2020, **190**, 122229.
- 15 J. Lin, H. Ma, Z. Wang, S. Zhou, B. Yan, F. Shi, Q. Yan, J. Wang, H. Fan and J. Xiang, *Macromol. Rapid Commun.*, 2021, **42**, 2100318.
- 16 M. R. Molla, P. Rangadurai, L. Antony, S. Swaminathan, J. J. de Pablo and S. Thayumanavan, *Nat. Chem.*, 2018, **10**, 659–666.
- 17 G. Mao, J. Wang, S. R. Clingman, C. K. Ober, J. T. Chen and E. L. Thomas, *Macromolecules*, 1997, **30**, 2556–2567.
- 18 Y. Tian, K. Watanabe, X. Kong, J. Abe and T. Iyoda, *Macromolecules*, 2002, **35**, 3739–3747.
- 19 Y. Sun, B. Xu, J. Li, Y. Wang, X. Li and S. Lin, *Mater. Chem. Front.*, 2022, **6**, 908–915.
- 20 S. Guan, Z. Deng, T. Huang, W. Wen, Y. Zhao and A. Chen, *ACS Macro Lett.*, 2019, **8**, 460–465.
- 21 Y. Zhu, C. Ma, H. Han, R. Sun, X. Liao and M. Xie, *Polym. Chem.*, 2019, **10**, 2447–2455.
- 22 E. Blasco, J. del Barrio, M. Piñol, L. Oriol, C. Berges, C. Sánchez and R. Alcalá, *Polymer*, 2012, **53**, 4604–4613.
- 23 W. C. Xu, S. Sun and S. Wu, *Angew. Chem., Int. Ed.*, 2019, **58**, 9712–9740.
- 24 H. Yu, T. Iyoda and T. Ikeda, *J. Am. Chem. Soc.*, 2006, **128**, 11010–11011.
- 25 S. Nagano, Y. Koizuka, T. Murase, M. Sano, Y. Shinohara, Y. Amemiya and T. Seki, *Angew. Chem., Int. Ed.*, 2012, **51**, 5884–5888.

- 26 Y. Morikawa, T. Kondo, S. Nagano and T. Seki, *Chem. Mater.*, 2007, **19**, 1540–1542.
- 27 S. Sun, C. Yuan, Z. Xie, W.-C. Xu, Q. Zhang and S. Wu, *Polym. Chem.*, 2022, **13**, 411–419.
- 28 F. Cai, T. Song, B. Yang, X. Lv, L. Zhang and H. Yu, *Chem. Mater.*, 2021, **33**, 9750–9759.
- 29 Y. Sun, F. Gao, Y. Yao, H. Jin, X. Li and S. Lin, *ACS Macro Lett.*, 2021, **10**, 525–530.
- 30 W. Wen and A. Chen, *Polym. Chem.*, 2021, **12**, 2447–2456.
- 31 W. Wen, W. Ouyang, S. Guan and A. Chen, *Polym. Chem.*, 2021, **12**, 458–465.
- 32 L. Ding, J. Li, T. Li, L. Zhang and W. Song, *React. Funct. Polym.*, 2017, **121**, 15–22.
- 33 L. Ding, M. Xu, J. Wang, Y. Liao and J. Qiu, *Polymer*, 2014, **55**, 1681–1687.
- 34 P. G. Cozzi, *Chem. Soc. Rev.*, 2004, **33**, 410–421.
- 35 K. Gupta and A. K. Sutar, *Coord. Chem. Rev.*, 2008, **252**, 1420–1450.
- 36 M. E. Belowich and J. F. Stoddart, *Chem. Soc. Rev.*, 2012, **41**, 2003–2024.
- 37 A. Chao, I. Negulescu and D. Zhang, *Macromolecules*, 2016, **49**, 6277–6284.
- 38 J. Hu, R. Mo, X. Sheng and X. Zhang, *Polym. Chem.*, 2020, **11**, 2585–2594.
- 39 H. Hu, L. Wang, L. Wang, L. Li and S. Feng, *Polym. Chem.*, 2020, **11**, 7721–7728.
- 40 W. Sheng, S. T. Nick, E. M. Santos, X. Ding, J. Zhang, C. Vasileiou, J. H. Geiger and B. Borhan, *Angew. Chem., Int. Ed.*, 2018, **57**, 16083–16087.
- 41 M. Wang, L. Xu, M. Lin, Z. Li and J. Sun, *Polym. Chem.*, 2021, **12**, 2825–2831.
- 42 N. Kalva, S. Uthaman, R. Augustine, S. H. Jeon, K. M. Huh, I. K. Park and I. Kim, *Macromol. Biosci.*, 2020, **20**, 2000118.
- 43 L. Greb, A. Eichhöfer and J.-M. Lehn, *Eur. J. Org. Chem.*, 2016, **2016**, 1243–1246.
- 44 L. Greb and J.-M. Lehn, *J. Am. Chem. Soc.*, 2014, **136**, 13114–13117.
- 45 E. Fischer and Y. Frei, *J. Chem. Phys.*, 1957, **27**, 808–809.
- 46 L. Greb, H. Mutlu, C. Barner-Kowollik and J.-M. Lehn, *J. Am. Chem. Soc.*, 2016, **138**, 1142–1145.
- 47 W. Jakubowski, B. Kirci-Denizli, R. R. Gil and K. Matyjaszewski, *Macromol. Chem. Phys.*, 2008, **209**, 32–39.
- 48 B. Droumaguet, *Chem. Commun.*, 2012, **48**, 1586–1588.
- 49 K. Matyjaszewski, K. Davis, T. E. Patten and M. Wei, *Tetrahedron*, 1997, **53**, 15321–15329.
- 50 K. Philipps, T. Junkers and J. J. Michels, *Polym. Chem.*, 2021, **12**, 2522–2531.
- 51 A. H. Ribeiro, J. Haven, A.-L. Buckinx, M. Beuchel, K. Philipps, T. Junkers and J. J. Michels, *Polym. Chem.*, 2021, **12**, 216–225.
- 52 Z. Grubisic, P. Rempp and H. Benoit, *Rubber Chem. Technol.*, 1969, **42**, 636–640.
- 53 P. Groves, *Polym. Chem.*, 2017, **8**, 6700–6708.
- 54 D. P. Valencia and F. J. González, *Electrochem. Commun.*, 2011, **13**, 129–132.
- 55 B. D. Mather, K. Viswanathan, K. M. Miller and T. E. Long, *Prog. Polym. Sci.*, 2006, **31**, 487–531.
- 56 W. Li and J. Wang, *Angew. Chem., Int. Ed.*, 2014, **53**, 14186–14190.